Journal of Theoretical and Applied Information Technology
20th December 2013. Vol. 58 No.2

ISSN: 1992-8645 www.jatit.org E-ISSN: 1817-3195

A NEW CORNER DETECTION METHOD FOR OMNIDIRECTIONAL IMAGES

[1] OMAR EL KADMIRI, [2] LHOUSSAINE MASMOUDI

[1, 2] LETS/Geomat Laboratory, Physics Department. Faculty of Science, Mohammed V University-Agdal, Morocco

E-mail: [1]omar.elkadmiri@gmail.com, [2]lhmasmoudi@gmail.com

ABSTRACT

Recently, many robotic applications adopted omnidirectional vision sensors. The achievement of those applications is usually based on computer vision algorithms by means of visual indices extraction from the acquired images, such as edge, region, and interest points detection. The use of classical image processing algorithms for omnidirectional images proved its limitations. Some new methods which take into account the special geometrical properties of omnidirectional images have been developed and used with success. Along these lines, this paper proposes a new corner detector more adequate for this class of images. The method is based on a virtual spherical electrostatic model for edge detection and the standard Harris corner detector. Experimental results and quantitative assessments affirm the performance of the proposed approach against several image degradations. Confrontation to other classical methods is provided.

Keywords: *Omnidirectional Vision, Corner Detection, Virtual Electrostatic Model, Harris Corner Detector, Visual Servoing.*

1. INTRODUCTION

1.1 Omnidirectional vision

Many techniques to improve the cameras field of view have been suggested in the literature [4,5], nevertheless the catadioptric approach still one of the most commonly adopted. By offering a wide field of view, catadioptric cameras are getting progressively more interest. Many computer vision applications such as video surveillance [1], autonomous navigation [2] and SLAM [3] are recently taking advantage of the great amount of visual information that can be provided by these sensors. Catadioptric cameras (Fig. 1) consist of a combination of convex mirrors (cata), lenses (dioptric) and standard cameras. Such optical solution offers a 360 degrees field of view (FOV) as well as instantaneous omnidirectional image acquisition (Fig.2).

We also opted for this approach. At the beginning of our research on omnidirectional vision, we designed and assembled some catadioptric vision systems. Images acquired with these sensors are not easy to interpret by the human visual system (Fig. 2 a), for that we presented in [13] an unwrapping algorithm of omnidirectional images valid for most catadioptric cameras and allowing generation of panoramic images such as the one shown in figure

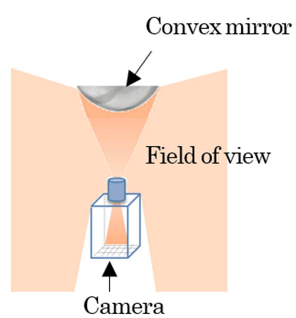

Fig. 1. Catadioptric Camera.

2.b. We noted that the privilege of a wide field of view provided by catadioptric imaging systems is supplied with significant radial distortions comprised in the acquired images. Furthermore these images are not uniformly sampled.

Classical image processing algorithms designed for perspective images such as edge or corner detection methods, commonly consider the input image as a uniform space, and the position of each pixel neighbors is known beforehand independently of its position in the image. Therefore these conventional image processing tools are not

Journal of Theoretical and Applied Information Technology
20th December 2013. Vol. 58 No.2

ISSN: 1992-8645 www.jatit.org E-ISSN: 1817-3195

appropriate for omnidirectional images. Hence the need of developing new image processing methods more adapted to the special particularities of such images.

(a)

(b)

Fig. 2. (A) Omnidirectional Image. (B) Unwrapped Panoramic Image.

Few interesting research studies have been done in this field. In [8] a SIFT (Scale Invariant Feature Transform) in the spherical coordinates for omnidirectional images was presented, experimental results confirm the promising and accurate performance of such algorithms. As well as authors of [9] have proposed an edge detection method adapted to omnidirectional images geometry, with Fuzzy sets used to take into account all imprecisions introduced by the sampling process allowing a coherent edge detection on these images. C. Demonceaux has proposed in [10] to define catadioptric image processing from the geodesic metric on the unitary sphere, which allows adapting classical image processing methods to catadioptric images. The efficiency of this approach was experimentally approved.

1.2 Corner Detection

Many computer vision applications such as visual servoing, localization tracking and pattern recognition use corner (interest points) detection as crucial step for reducing the large amount of input data to a set of features (fig. 3). Usually interest points denote geometric discontinuities, while corners are a special case of them. A corner can refer to an intersection of at least two main and distinct edges.

Fig. 3. Corner detection in a panoramic image.

Various corner detection approaches have been developed in the literature. They can be classified into three major categories: Edge based corner detectors, Graylevel derivative corner detectors, and direct graylevel detectors.

In 1977 Moravec has proposed a corner detection method based on self-similarity measurement by sum of square differences (SSD). This method have been improved later by Harris and Stephens [6] using a local auto-correlation function. The proposed cornerness measure is given as follows:

$$C(x,y) = \det(M) - k(trace(M))^2 \quad (1)$$

Where M = $\begin{bmatrix} A & C \\ C & B \end{bmatrix}$, $det(M) = \lambda_1\lambda_2 = AB - C^2$.

And $trace(M) = \lambda_1{+}\lambda_2 = A + B$, k is a constant. A, B and C are defined as:

$$A = \left(\frac{dI}{dx}\right)^2 \otimes w \quad (2)$$

$$B = \left(\frac{dI}{dy}\right)^2 \otimes w \quad (3)$$

And $C = \left(\frac{dI}{dx}\frac{dI}{dy}\right) \otimes w \quad (4)$

w denotes the weight of the Gaussian smoothing window.

Matrices A, B and C are commonly calculated using first order gradient which is estimated using classical derivation masks as an edge detection method. Then local maxima search process is carried out as a final step of Harris corner detection algorithm. It is noteworthy that the robustness of the edge detection process affects significantly the performance of corners detection.

In [7] we developed an edge detection operator specially designed for omnidirectional images. It

ISSN: 1992-8645 www.jatit.org E-ISSN: 1817-3195

was based on a spherical virtual electrostatic charges distribution model. Experimental results have proved that the proposed edge detection operator respects the geometrical properties of catadioptric images, besides it's robustness against noise. In this article we propose a new corner detection approach in catadioptric images, combining the former edge detection operator with Harris corner detection method. The proposed algorithm will be detailed in section II, then experimental results and quantitative assessments are discussed in section III.

2. CORNER DETECTION IN SPHERICAL IMAGES

2.1 A spherical edge detection operator

As mentioned in the introduction, commonly simple gradient masks are used to compute $\boldsymbol{dI/dx}$ and $\boldsymbol{dI/dy}$ derivatives of the input image, used in (2), (3) and (4) as a first step of Harris corner detection algorithm.

Whereas it is well known that edge detection methods based on gradient kernels are more sensitive to noise. We propose to replace those kernels by an edge detection operator which was based on a spherical virtual electrostatic model more adapted to catadioptric images geometry and less sensitive to noise.

This modeling was presented in details in [7]. It consists of considering the catadioptric image as a spherical grid of charged particles distributed on a spherical surface in electrostatic equilibrium.

Then the image can be divided into 3 x 3 pixels blocks (Fig. 4). We assume that forces exerted by charges beyond the 3x3 window on the central charge are neglected. The succeeding analogy is made: pixels intensity matches to electric charges values, and the central charge is exposed to the electrostatic forces of all eight neighboring charges.

The final expressions of exerted forces are given by:

$$\overrightarrow{F_\varphi} = k'q_0 \frac{1}{(sin(\theta)d\varphi)^2}\left[q_5 - q_1 + \frac{\sqrt{2}}{4}(q_6 - q_2 + q_4 - q_8)\right] \vec{e}_\varphi \quad (5)$$

$$\overrightarrow{F_\theta} = k'q_0 \frac{1}{(sin(\theta)d\varphi)^2}\left[q_3 - q_7 + \frac{\sqrt{2}}{4}(q_2 - q_6 + q_4 - q_8)\right] \overrightarrow{e_\theta} \quad (6)$$

Where k' is a constant defined by: $1/4\pi\varepsilon_0 \mathrm{R}^2$

Let $p(i,j) = q_0$ be the central pixel defined on the studied block, we obtain the two following edge detection filters G_φ and G_θ toward φ and θ directions defined as:

$$G_\varphi = 1/(sin(\theta)\, d\varphi)^2 \begin{pmatrix} \sqrt{2}/4 & 0 & -\sqrt{2}/4 \\ 1 & 0 & -1 \\ \sqrt{2}/4 & 0 & -\sqrt{2}/4 \end{pmatrix} \quad (7)$$

$$G_\theta = 1/\, sin(\theta)\, d\varphi)^2 \begin{pmatrix} \sqrt{2}/4 & 1 & \sqrt{2}/4 \\ 0 & 0 & 0 \\ -\sqrt{2}/4 & -1 & -\sqrt{2}/4 \end{pmatrix} \quad (8)$$

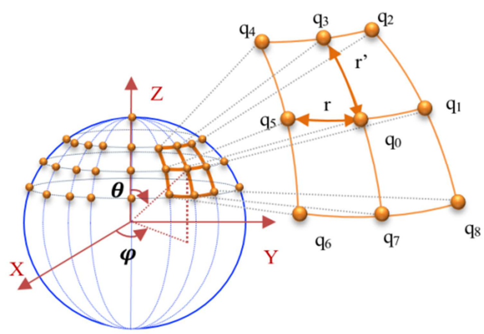

Fig. 4. Spherical Electric Charges Distribution.

In the case of singularity where $\theta = 0$, which represents the case of the north Pole, a value of 0.001 is affected to θ.

2.2 Processing spherical images

The sphere is a suitable space for processing catadioptric images. Forasmuch as their mapping on the sphere respects the correct positioning of each pixel neighbors during the processing. This is well illustrated in Figure 5 showing the manner in which planar and spherical filters convolute a catadioptric image.

So we propose to map catadioptric images on the sphere using stereographic projection. This transformation remains mathematically valid; As Geyer and Daniilidis have proved in [11] that generally catadioptric images can be mapped bijectively on the sphere.

Stereographic projection is defined in geometry as a bijective mapping transformation projecting the sphere onto a plane. This conformal projection is defined on the sphere deprived of one point called: projection point. The equatorial plane is the one separating the two north and

Journal of Theoretical and Applied Information Technology
20th December 2013. Vol. 58 No.2

ISSN: 1992-8645 www.jatit.org E-ISSN: 1817-3195

south hemispheres. Stereographic projection can be made on any plane parallel to the equatorial one. In our case the tangent plane on the North Pole is chosen as the projection plane.

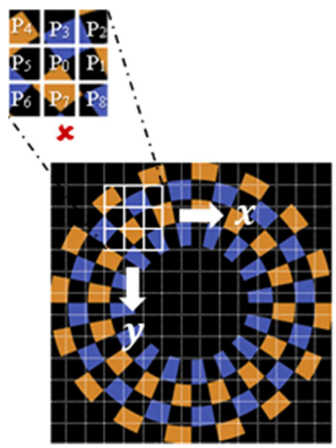

(a)

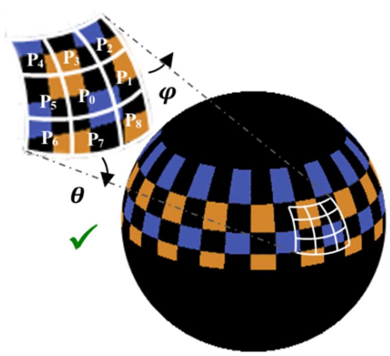

(b)

Fig. 5. (A): Incorrect Neighboring Pixels In The Case Of Planar Filters. (B): Correct Neighboring Pixels In The Case Of Spherical Filters.

In three-dimensional space $\mathbb{R}3$, the sphere is defined as a set of points with three-dimensional vector:

$$P = (x_0, x_1, x_2) = (r\cos\theta, r\sin\theta\sin\varphi, r\sin\theta\cos\varphi) \quad (9)$$

With $r \in [0, \infty]$, $\theta \in [0, \pi]$ and $\phi \in [0, 2\pi]$.

The stereographic projection is performed from the South Pole. Allowing projecting any point of the sphere onto the tangent plane at the North Pole (Fig. 6).

Considering the sphere $S2$ as the Riemannian sphere $(R = 1)$ and the tangent plane as the complex plane $\mathbb{C}^2$, then the stereographic projection is a bijection given by:

$$\tau(p) = 2\tan\frac{\theta}{2}(\cos\varphi; \sin\varphi) \quad (10)$$

Where $p = (\theta, \varphi)$, $\theta \in [0, \pi]$, $\varphi \in [0, 2\pi]$.

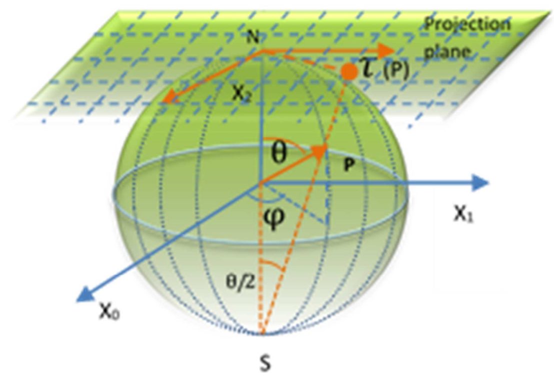

Fig. 6. : South Polar Stereographic Projection.

As a first step of our corner detection algorithm, the catadioptric image $I(u, v)$ is mapped through inverse stereographic projection to $I_s(\theta, \varphi)$ on the sphere. Then convolution with our developed edge detection spherical kernels $G_s(\theta, \varphi)$ is performed directly on the sphere. The next step consists of computing the auto-correlation matrix M at each image pixel, as defined in the introduction. Then the cornerness measure $C(\theta, \varphi)$is calculated in order to determine local maxima which define corners.

We notice that the hessian matrix in spherical coordinates is given by:

$$M = \begin{bmatrix} I_{\theta\theta} & I_{\theta\varphi} \\ I_{\varphi\theta} & I_{\varphi\varphi} \end{bmatrix} \quad (11)$$

And Gaussian smoothing window is calculated using the following equation:

$$G = \frac{1}{2\pi\sigma^2} e^{-d/2\sigma^2} \quad (12)$$

Where d is the distance separating the central pixel $p_c(\theta_c, \varphi_c)$ from its neighbor $p_n(\theta_n, \varphi_n)$ given by:

$$d = arc\cos(\sin\varphi_c \sin\varphi_n + \cos\varphi_c \cos\varphi_n \cos(\theta_n - \theta_c)) \quad (13)$$

Finally the output image $O(\theta, \varphi)$ is stereographically projected onto $O(u, v)$ on the plane (Fig. 7).

jatit.org E-ISSN: 1817-3195

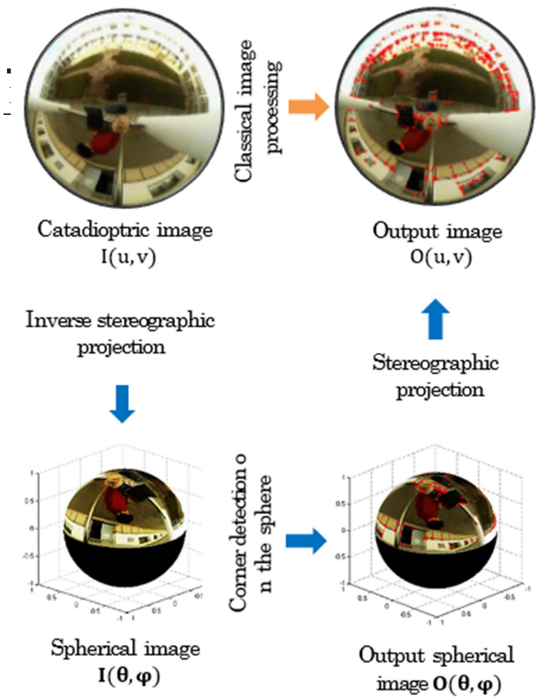

Fig. 7. Corner Detection Algorithm In Catadioptric Images.

3. EVALUATION CRITERIONS

A good corner detection algorithm must satisfy several requirements

- Robustness against noise and image degradations.
- Detection of maximum true corners.
- Good localization of detected corners.
- Minimum detection of false corners.

In order to evaluate our proposed corner detection algorithm a set of synthetic images was generated. Those artificial images have the same properties of real catadioptric ones, including radial distortion. At each conducted experiment, the proposed corner detection algorithm operating on the sphere was confronted to standard Harris corner detection algorithm operating on the plane, and using Sobel method as an edge detection operator.

We quantitatively evaluate each detector by calculating three scores inspired from biometrics performance evaluation methods [12]:

The False Rejection Rate, we define as:

$$FRR = \frac{u_c}{t_c} \quad (14)$$

Where u_c the number of true undetected corners, and t_c is the total corners number. The False Acceptance Rate:

$$FAR = \frac{f_c}{t_p} \quad (15)$$

f_c the number of false detected corners, and t_p is the total number of all detected points, and the Total Error Rate defined as:

$$TER = \frac{u_c + f_c}{t_c + t_p} \quad (16)$$

Let us note that, in order to ensure an objective assessment we used the same Gaussian smoothing coefficient σ equal to 1.5 for both detectors at each experiment. Since the choice of an appropriate value of this coefficient still an open problem.

4. EXPERIMENTAL RESULTS AND DISCUSSION

In this section we present the experimental results on several synthetic and real omnidirectional images. Both, classical Harris corner detector and the proposed method are confronted.

Our first experiment applies the proposed algorithm to a graylevel synthetic images. The first omnidirectional image with 2180x2180 pixels include two classes with intensity values of 0 and 204 (see figure 8). To test the algorithm performance under different resolution levels and diverse total number of corners, a second synthetic omnidirectional image shown in figure 11 was considered, with a resolution of 2390x2390, and including the same classes of the first image.

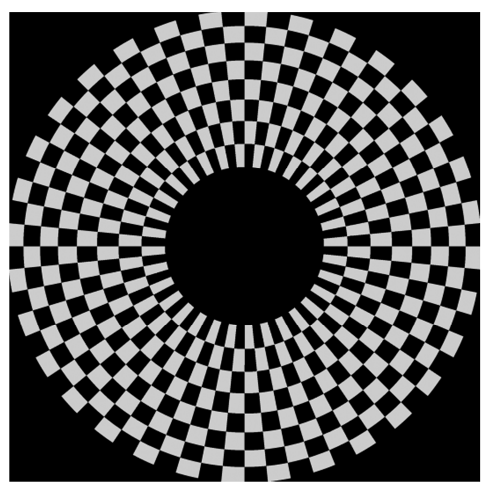

Fig. 8. First Original Synthetic Omnidirectional Image.

Figures 9 and 10 below illustrate the obtained results using the first synthetic image for both evaluated methods. Then Table 1 gives the corner detection accuracy.

Journal of Theoretical and Applied Information Technology
20th December 2013. Vol. 58 No.2

ISSN: 1992-8645 www.jatit.org E-ISSN: 1817-3195

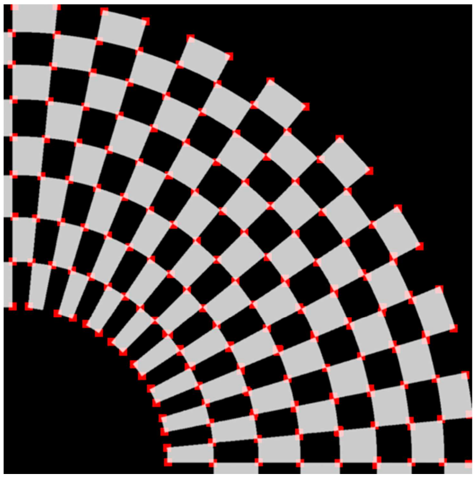

Fig. 9. Corner Detection Result Using The Proposed Approach.

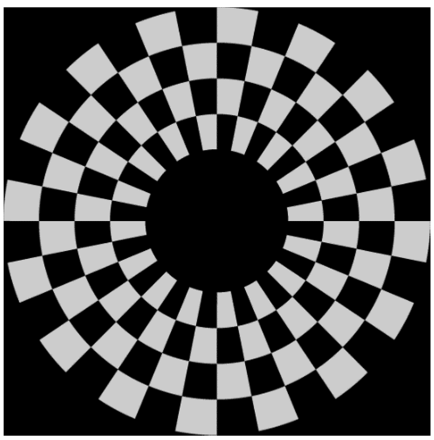

Fig. 10. Corner Detection Result Using Standard Harris Detector.

Table 1. Evaluation Scores for the first synthetic image.

	Proposed approach	Standard Harris
FRR	0.65%	6.63%
FAR	18.71%	44.78%
TER	10.58%	30.58%

Figure 11, is the second synthetic omnidirectional image. Related results are given below.

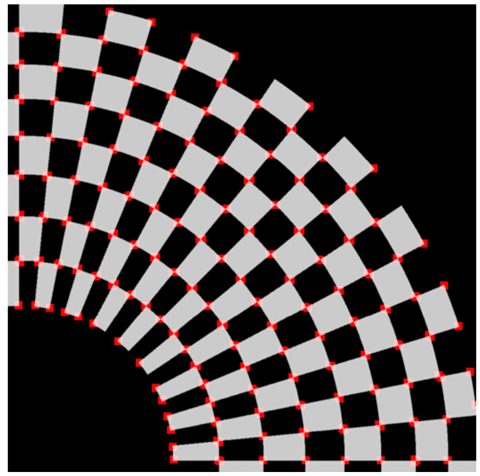

Fig. 11. Second Synthetic Omnidirectional Image.

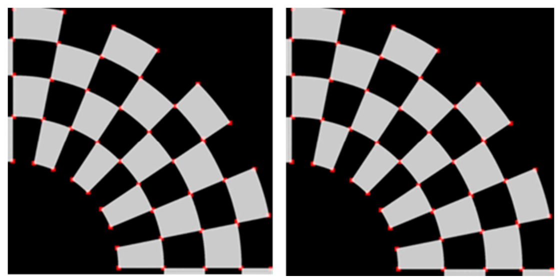

(a) The proposed approach (b) Standard Harris.

Fig. 12. Corner Detection Results In The Second Synthetic Image.

Table 2. Evaluation Scores For The Second Synthetic Image.

	Proposed approach	Standard Harris
FRR	0%	11.11%
FAR	8.16%	42.02%
TER	4.25%	29.82%

In order to study the behavior of the proposed corner detection method against several image degradations, initially the second artificial omnidirectional image was corrupted with a Gaussian noise with zero mean and 0.01 variance. We obtained the following results:

ISSN: 1992-8645 www.jatit.org E-ISSN: 1817-3195

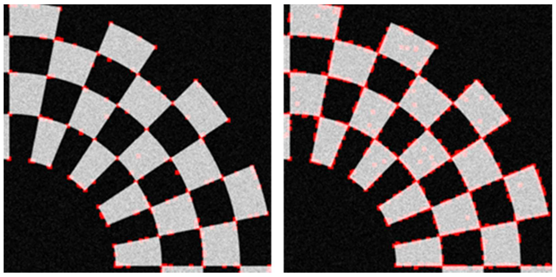

(A) The Proposed Approach (B) Standard Harris.

Fig. 13. Corner Detection Results In A Noised Synthetic Image.

Table 3. Evaluation Scores: Gaussian Noise.

	Proposed approach	Standard Harris
FRR	0%	6.66%
FAR	68.53%	92.02%
TER	52.12%	85.28%

Then we simulate a blurred image that might be result of camera motion by nine pixels, with an angle of 0 degrees in a counterclockwise direction. The results are as follows:

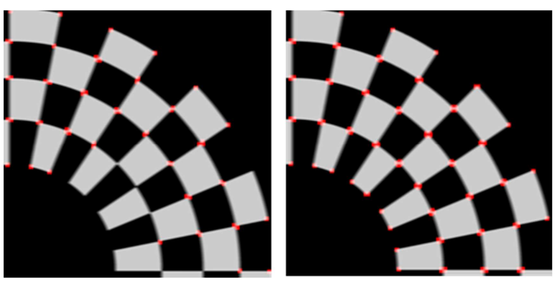

(a) The proposed approach (b) Standard Harris.

Fig. 14. Corner Detection Results In A Blurred Synthetic Image.

Table 4. Evaluation Scores: Motion Blur.

	Proposed approach	Standard Harris
FRR	24.44%	4.44%
FAR	44.26%	67.18%
TER	35.84%	51.13%

Evaluation of detected corners localization is carried out using Euclidean distance metrics between real corners position, and detected ones by each detector. Reminding that this Euclidean distance considering two pixels $p(u_p, v_p)$ and $q(u_q, v_q)$, is calculated using the following equation:

$$d = \sqrt{(u_p - u_q)^2 + (v_p - v_q)^2} \quad (17)$$

A synthetic image block of nine corners was considered, obtained results are as following:

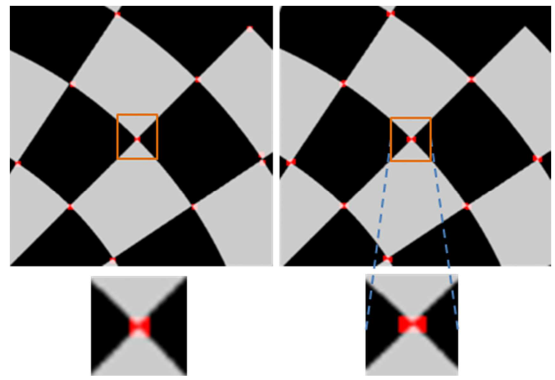

(A) The Proposed Approach (B) Standard Harris.

Fig. 15. Euclidean Metric Results.

Table 5. Euclidean Metric Results.

	Proposed approach	Standard Harris
d	2.15	2.96

It can be seen from table 1 that the FRR and FAR of classical Harris corner detector are higher than those of the proposed approach. This can be explained by the fact that the classical detector tends to detect a high amount of double corners (Higher FAR), while ignoring some real corners (Higher FRR).

These same observations were confirmed while performing both methods on a second synthetic catadioptric image (see Fig. 12).

The influence of using non-gradient based edge detection kernels was very noticeable when we processed a noisy image. Results shown in table 3 proved that the proposed approach is more stable against noise.

Considering the TER (Total Error Rate), in the case of a blurred image (Fig. 14) the proposed approach remains providing better results than the classical one.

From table 5, we can see the relative enhancement of localization accuracy by the proposed method.

Secondly, other experimentation has been conducted on real catadioptric images.

Journal of Theoretical and Applied Information Technology
20th December 2013. Vol. 58 No.2

ISSN: 1992-8645 www.jatit.org E-ISSN: 1817-3195

An indoor scene including a black and white checkerboard was acquired with our catadioptric camera, with the aim of evaluating the detector in real conditions of use. Obtained results are given in figures below.

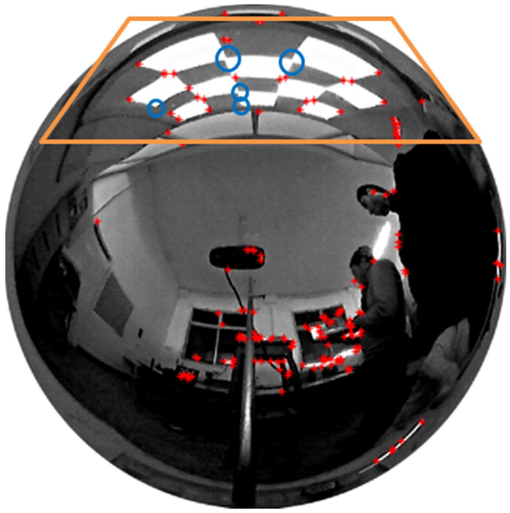

Fig. 16. Corner Detection Result In A Real Omnidirectional Image, By Standard Harris Method.

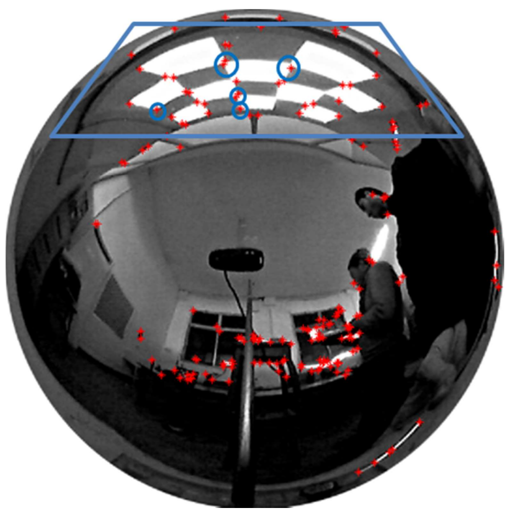

Fig. 17. Corner Detection Result In A Real Catadioptric Image, By The Proposed Method.

Conducted experiments for real catadioptric images (Figures 16,17) confirms that the robustness of the proposed approach against noise is not simply due to an intrinsic smoothing effect; seeing that in the case of a real scene of a checkerboard, five true corners (see blue circles) was missed by the classical approach, while they were detected by the spherical one. In other words the efficiency of the proposed detector against various noise forms does not affect its false rejection rate and it still providing a good compromise between criterions characterizing a good corner detection algorithm as they were mentioned in section III. The last illustration of provided results was obtained on a real catadioptric image containing a calibration pattern, shown in figure 18.

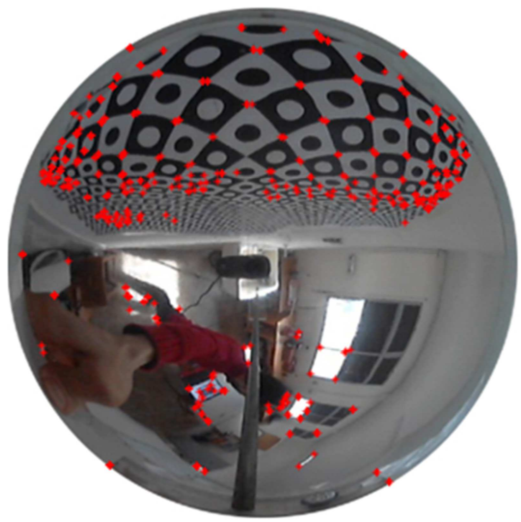

Fig. 18. Corner Detection Result In A Real Catadioptric Image, By The Proposed Method.

This study is part of an ongoing research project aiming feature-based visual servoing of mobile robots using an omnistereo vision system similar to the one we presented in [14] but more compact, and allows instantaneous stereo omnidirectional images acquisition.

Feature-based vision systems are only effective when good features can be detected and tracked from frame to frame. In [15] a good performance assessment of corner feature detecting algorithms for future tracking applications has been presented.

Until now we developed a real time color based tracking algorithm robust under varying illumination, embedded on a mobile robot (see figure 19). Since the obtained results with the presented corner detection method are promising, we project to integrate it into the former object tracking algorithm. Through this the tracker will be able to identify robustly an object by its color and its shape. Figure 20 is given as an illustration of detected corners after color segmentation and threshold of a tracked object.

Journal of Theoretical and Applied Information Technology
20th December 2013. Vol. 58 No.2

ISSN: 1992-8645 www.jatit.org E-ISSN: 1817-3195

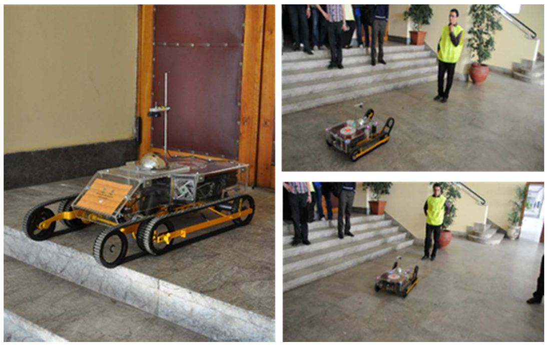

Fig. 19. ESCALADE360: A Mobile Robot With An Omnidirectional Camera Performing Real Time Object Tracking.

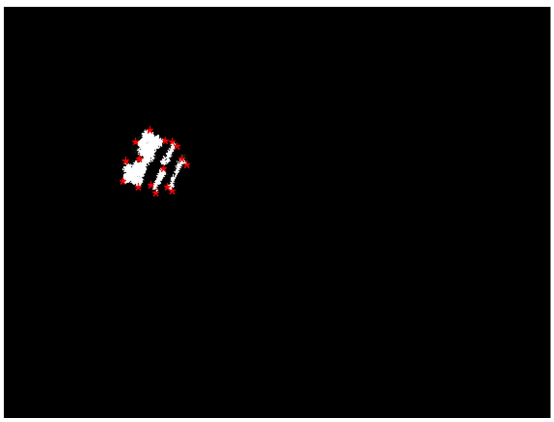

Fig. 20. Detected Corners After Color Segmentation And Thresholding On A Real Omnidirectional Image.

5. CONCLUSION

We developed a new corner detection method for omnidirectional image. By respecting the correct positioning of processed pixels this method provides improved results than the standard ones. And being non-gradient based, it guarantee a more stable performance against various image degradation especially noise. These findings were confirmed by a subjective evaluation study, and a confrontation to classical corner detection methods.

REFRENCES:

[1] Chen, C.-H., Yao, Y., Page, D., Abidi, B., Koschan, A., Abidi, M.. "Heterogeneous Fusion of Omnidirectional and PTZ Cameras for Multiple Object Tracking", IEEE Transactions on Circuits and Systems for Video Technology 18, p. 1052, (2003).
[2] N. Winters, J. Gaspar, G. Lacey, J. Santos-Victor, "Omni-directional vision for robot navigation," Proceedings of IEEE Workshop on Omnidirectional Vision, pp. 2128. (2000).
[3] A. Rituerto, Puig, J. J. Guerrero, "Comparison of omnidirectional and conventional monocular systems for visual slam," 10th Workshop on Omnidirectional Vision, Camera Networks and Non-classical Cameras, OMNIVIS 2010, Zaragoza, Spain.
[4] Y. Xiong, K. Turkowski, "Creating image based vr using a selfcalibrating fisheye lens," In CVPR97, pages 237--243, (1997).
[5] T. Sato et N. Yokoya, "Omni-directional Multi-baseline Stereo without Similarity Measures," IEEE Workshop on Omnidirectional Vision and Camera Networks (OMNIVIS 2005), (October, 2005).
[6] C. Harris and M. Stephens. "A combined corner and edge detector," Proceedings of the 4th Alvey Vision Conference. pp. 147–151, (1988).
[7] O. El kadmiri, Z. El kadmiri, L. Masmoudi "A Spherical Electrostatic Model Edge Detector For Omnidirectional Images" Journal of Theoretical and Applied Information Technology. Vol. 51, (May 2013).
[8] J. Cruz-Mota, I. Bogdanova, B. Paquier, M. Bierlaire, J.P. Thiran "Scale Invariant Feature Transform on the Sphere: Theory and Applications". International Journal of Computer Vision (10 November 2011), pp. 1-25.
[9] F. Jacquey, F. Comby, O. Strauss, "Fuzzy edge detection for omnidirectional images," Fuzzy Sets and Systems, Volume 159, Issue 15, 1 August 2008, Pages 1991-2010.
[10] Cédric Demonceaux, Pascal Vasseur, and Yohan Fougerolle. 2011. "Central catadioptric image processing with geodesic metric," Image Vision Comput. 29, 12 (November 2011), 840-849.
[11] C. Geyer and K. Daniilidis, "Catadioptric projective geometry," International Journal of Computer Vision, Vol. 45, No. 3, pp. 223-243, (2001).
[12] Kar-Ann Toh, Jaihie Kim, and Sangyoun Lee. "Biometric scores fusion based on total error rate minimization," Pattern Recogn. 41, 3 (March 2008), 1066-1082.
[13] O. El Kadmiri and L. Masmoudi, "An omnidirectional image unwrapping approach," International Conference on Multimedia Computing and Systems (ICMCS), (7-9 April 2011).
[14] Z. El Kadmiri, O. El Kadmiri, and L. Masmoudi. "Depth Estimation For Mobile Robot Using Single Omnidirectional Camera System," Journal of Theoretical and Applied Information Technology 44, no. 1, (2012).
[15] P. Tissainayagam, & D. Suter. "Assessing the performance of corner detectors for point feature tracking applications," Image and Vision Computing, 22(8), 663-679, (2004).